



ARTICLE

Biobased Furfurylated Poplar Wood for Flame-Retardant Modification with Boric Acid and Ammonium Dihydrogen Phosphate

Ming Ni¹, Lei Li¹, Yiqiang Wu^{1,*}, Jianzheng Qiao¹, Yan Qing¹, Ping Li² and Yingfeng Zuo^{1,*}

¹College of Materials Science and Engineering, Central South University of Forestry and Technology, Changsha, 410004, China

²College of Furniture and Art Design, Central South University of Forestry and Technology, Changsha, 410004, China

*Corresponding Authors: Yiqiang Wu. Email: wuyq0506@126.com; Yingfeng Zuo. Email: zuoyf1986@163.com

Received: 17 May 2024 Accepted: 29 May 2024 Published: 06 September 2024

ABSTRACT

Furfurylated wood exhibits excellent dimensional stability and corrosion resistance, making it a promising material for constructing buildings, but it is highly flammable. Herein, flame-retardant furfurylated poplar wood was produced via a two-step process utilizing boric acid (BA) and ammonium dihydrogen phosphate (ADP) as flame-retardant components, and biomass-derived furfuryl alcohol (FA) as a modifier. The acidity of BA and ADP allowed them to catalyze the polymerization of FA, which formed a cross-linked network that immobilized BA and ADP inside the wood. The addition of BA/ADP substantially delayed the time to ignition from 10 to 385 s and reduced the total heat release and total smoke release by 58.75% and 77.31%, respectively. Analysis of the pyrolysis process showed that the decomposition products of BA and ADP protected the underlying furfurylated wood and diluted combustible gases. This method significantly improved the fire retardancy and smokeless properties of furfurylated wood, providing promising prospects for its application as an engineering material.

KEYWORDS

Poplar wood; furfuryl alcohol; furfurylated wood; flame retardancy; boric acid; ammonium dihydrogen phosphate

1 Introduction

With the depletion of fossil resources and worsening environmental problems in recent years, the use of alternative renewable resources has emerged as a promising solution to ensure ecological development [1]. As one of the most abundant biomaterials on Earth, wood presents a multifaceted solution to the challenges of sustainable development [2]. Fast-growing forests are playing an increasingly important role in ensuring a steady supply of wood, which is becoming threatened due to the overexploitation of forests [3]. However, fast-growing woods have low dimensional stability and flammability, limiting their use as engineering materials and making it necessary to modify them to enhance their properties.

Most wood modification methods use non-renewable chemicals and produce harmful byproducts that reduce the environmental friendliness of modified wood [4]. Furfuryl alcohol, a green platform compound [5], is synthesized through the catalytic hydrogenation of furfural in either gaseous or liquid phases [6]. Furfural can be produced by the cracking and dehydration of pentose from agricultural waste such as corn cobs, sugarcane bagasse, and rice husks [7]. The furfurylation of wood has garnered significant



interest from both academic and industrial sectors due to furfuryl alcohol's reputation as an environmentally sustainable wood modifier.

The furfurylation of wood is a complex chemical reaction. When heated in the presence of a catalyst, furfuryl alcohol polymerizes in wood cells to form a cross-linked furfuryl alcohol polymer [8], which has been shown to significantly improve the dimensional stability [9,10] and durability [11] of wood. At the same time, the density and hardness of the wood are improved. Furfuryl alcohol can also protect wood from degradation by marine organisms [12], but furfuryl alcohol resins increase the flammability of wood [13]. After modification with furfuryl alcohol, the total heat release of poplar wood increased by 21.36%, the peak heat release rate increased by 29.49%, and the flame intensity during combustion was significantly higher [14]. Some studies have added ammonium dihydrogen phosphate [14], montmorillonite [15], or guanidylurea phosphate [16] to furfuryl alcohol solution to improve the flame retardancy of furfurylated wood. However, after adding a flame retardant, the modification solution readily stratified, which greatly shortened the storage period.

In this work, we used a two-step method to prepare fire-retardant furfuryl alcohol-modified wood. Boric acid and ammonium dihydrogen phosphate were deposited in the wood, which was then modified with furfuryl alcohol. This method circumvents the necessity for the miscibility of furfuryl alcohol and the flame retardant, mitigating stratification caused by premature catalytic polymerization of furfuryl alcohol, and enhances the loading capacity of the flame retardant. The acidity of boric acid and ammonium dihydrogen phosphate promoted the polymerization of furfuryl alcohol [13], which fixed the flame retardant inside the wood. The distribution of furfuryl alcohol resin and flame retardant in wood, the fixation properties, and the flame retardant and smoke suppression properties of modified wood were analyzed.

2 Materials and Methods

2.1 Materials

Poplar wood (*Populus tomentosa* Carr., Salicaceae) was sourced from Hunan Province, China. The poplar trees, aged 10 years and approximately 20 cm in diameter, were sawn into boards. Boards with smooth surfaces, free of burrs, scars, and decay, were selected for drying. These boards were then machined into the specified specimen sizes. 40 samples, each measuring $20 \times 20 \times 20 \text{ mm}^3$ ($L \times T \times R$), were prepared to test the liquid absorption rate, weight percent gain, bulking rate, density increase rate, and leachability. Four experiments were conducted, with each group consisting of 10 samples. 32 samples, each measuring $30 \times 20 \times 20 \text{ mm}^3$ ($L \times T \times R$), were prepared to test the compressive strength. Four sets of experiments were performed, with each group repeated 8 times. 24 samples, each measuring $300 \times 20 \times 20 \text{ mm}^3$ ($L \times T \times R$), were prepared to test the bending strength. Four experiments were conducted, with each group consisting of 6 samples. 24 samples, each measuring $70 \times 50 \times 50 \text{ mm}^3$ ($L \times T \times R$), were prepared to test the hardness. Four experiments were conducted, with each group consisting of 6 samples. 12 samples, each measuring $100 \times 10 \times 100 \text{ mm}^3$ ($L \times T \times R$), were prepared for cone calorimetry. Four sets of experiments were performed, with each group repeated 3 times. Before treatments, all wood samples were dried to a constant weight m_0 (g) and dimensions (L_0 , T_0 , R_0) in an oven at 103°C .

Furfuryl alcohol (FA, $\text{C}_5\text{H}_6\text{O}_2$, purity $\geq 98.5\%$), maleic anhydride (MA, $\text{C}_4\text{H}_2\text{O}_3$, purity $\geq 99.5\%$), sodium tetraborate ($\text{Na}_2\text{B}_4\text{O}_7 \cdot 10\text{H}_2\text{O}$, purity $\geq 99.5\%$), boric acid (BA, H_3BO_3 , purity $\geq 99.5\%$), and ammonium dihydrogen phosphate (ADP, $\text{H}_6\text{NO}_4\text{P}$, purity $\geq 99.0\%$) were purchased from Sinopharm Chemical Reagent Co., Ltd. (Shanghai, China). Deionized water was used as the solvent of the impregnation solutions.

2.2 Preparation of Impregnation Solutions

The water-based impregnation solutions included the BA/ADP treatment solution and the FA treatment solution. The BA/ADP treatment solution was formulated by sequentially incorporating BA (4 wt%) and ADP (16 wt%) into deionized water and stirring continuously. The FA treatment solution was prepared by successively adding MA (2 wt%), sodium tetraborate (2 wt%), and FA (30 wt%) to deionized water and stirring continuously.

2.3 Preparation of Furfurylated Wood

The modified wood samples were prepared using a two-step process with a vacuum pressure impregnation tank. In the first step, BA/ADP treatment solutions were used to impregnate the wood samples at -0.1 MPa for 30 min, followed by 0.5 MPa for 2 h. After impregnation, the samples were dried at 80°C for 24 h in an oven, and labeled as Wood-BA/ADP. In the second step, FA treatment solutions were impregnated into the Wood-BA/ADP using the same method. After impregnation, wipe off any excess liquid from the surface of the sample, weigh it as m_1 (g), wrap it in aluminum foil, and bake it in an oven at 103°C for 2 h. Then, remove the aluminum foil. The samples were dried at 80°C to a constant weight m_2 (g) and dimensions (L_1 , T_1 , R_1) and then labeled as Wood-BA/ADP-PFA. For comparison, the wood samples treated only with the second step were labeled as Wood-PFA.

2.4 Physical and Mechanical Properties

The liquid absorption rate (LAR), weight percent gain (WPG), bulking rate (BR), density increase rate ($\Delta\rho$), and leachability were calculated according to Eqs. (1) to (7). In these formulas, ρ_0 and ρ_1 represent the density of wood samples before and after modification, respectively. Additionally, m_3 denotes the absolute dry mass of the modified wood after a 14-day soaking period.

$$LAR (\%) = (m_1 - m_0)/m_0 \times 100\% \quad (1)$$

$$WPG (\%) = (m_2 - m_0)/m_0 \times 100\% \quad (2)$$

$$BR (\%) = [(L_1 \times T_1 \times R_1) - (L_0 \times T_0 \times R_0)]/(L_0 \times T_0 \times R_0) \times 100\% \quad (3)$$

$$\rho_0 (\text{kg/m}^3) = m_0/(L_0 \times T_0 \times R_0) \times 1000000 \quad (4)$$

$$\rho_1 (\text{kg/m}^3) = m_2/(L_1 \times T_1 \times R_1) \times 1000000 \quad (5)$$

$$\Delta\rho (\%) = (\rho_1 - \rho_0)/\rho_0 \times 100\% \quad (6)$$

$$Leachability (\%) = (m_2 - m_3)/(m_2 - m_0) \times 100\% \quad (7)$$

The compressive strength, bending strength, and hardness were tested according to the Chinese national standard GB/T 1927.11–2022, GB/T 1927.9–2021 and GB/T 1927.19–2021, respectively, using an MWD-W10 universal mechanical testing machine (Jinan Test Gold Group Co., Ltd., China). The compressive strength test involves positioning the sample at the center of the testing machine support table and applying a load at a uniform speed of 3.5 mm/min. The load is recorded when a significant reduction in load is indicated by the test machine. For the bending strength test, the sample is placed on two supports of the testing machine, with a distance of 240 mm between them. The indenter above the device destructs the sample at a uniform speed of 10 mm/min, and the load at this point is recorded. In the hardness test, the sample is positioned on the support of the testing machine, and the hemispherical steel indenter of the test equipment is brought to the center of the sample's test surface. The indenter is pressed into the test

surface of the sample at a uniform speed of 5 mm/min until the pressing depth reaches 5.64 mm, and the load at this point is recorded.

2.5 Stereoscopic Microscope

The morphological properties of the samples were observed using a stereoscopic microscope (AO-HK830-5870, AOSVI, Shenzhen, China).

2.6 Scanning Electron Microscope (SEM)

Scanning electron microscopy (MIRA LMS, TESCAN, Shanghai, China) and energy-dispersive X-ray spectroscopy (EDX) were employed to observe the micromorphology of the samples under vacuum mode with a 15 kV acceleration voltage. The samples were cut into slices measuring $10 \times 10 \times 3 \text{ mm}^3$ and dried to absolute dryness. Prior to observation, the samples were sputter-coated with gold to obtain clearer images.

2.7 X-Ray Photoelectron Spectroscopy (XPS)

The chemical compositions of the samples were obtained using an X-ray photoelectron spectrometer (K-Alpha, Thermo Fisher Scientific, USA) using monochromatic Al-K α radiation (1486.6 eV).

2.8 Fourier-Transform Infrared (FTIR) Spectroscopy

FTIR spectroscopy (Nexus 670, Thermo Fisher Scientific, USA) was used to identify the functional groups of samples. The test samples were homogeneous mixtures made from absolutely-dry wooden powder and KBr (1:100). The scanning wavenumber range was 400–4000 cm^{-1} , with a resolution of 4.0 cm^{-1} , and 16 scans were acquired per spectrum.

2.9 X-Ray Diffraction (XRD)

The crystal structures of the samples were inspected using an X-ray diffractometer (Empyrean, Malvern Analytical, UK). The scanning range was 5°–40°, and the scanning rate was 2°/min.

2.10 Thermogravimetric (TG) Analysis

The thermal stability of the samples was evaluated using thermogravimetric analysis (Pyris 6 TGA, Perkin Elmer, USA). The temperature during the test was ramped from room temperature to 800°C at a heating rate of 10°C/min. The test atmosphere was nitrogen with a gas flow rate of 20 mL/min.

2.11 Cone Calorimetry

Flame retardant and smoke suppression properties of the samples were tested using a cone calorimeter (FTT 0007, Fire Testing Technology) in accordance with ISO 5660-1: 2015. Samples with dimensions of $100 \times 10 \times 100 \text{ mm}^3$ ($L \times T \times R$) were tested for combustion under a heat flux of 50 kW/m². The main fire response parameters obtained included the time to ignition (TTI), heat release rate (HRR), peak heat release rate (PHRR), mean heat release rate (MHRR), total heat release (THR), smoke production rate (SPR), total smoke release (TSR), CO yield (COY), mean CO yield (MCOY), CO₂ yield (CO₂Y), mean CO₂ yield (MCO₂Y), and carbon residue ratio.

2.12 Statistical Analysis

Collected data were statistically evaluated using the Minitab Version 15 statistical software package and reported as the mean \pm standard deviation of replicates. Fisher's least significant difference (LSD) was used for ANOVA analysis to determine the significance of differences between mean values according to the minimum significance difference criterion at a 95% confidence level ($p < 0.05$).

3 Results and Discussion

3.1 Impregnation Effect

The liquid absorption rate (LAR), weight percent gain (WPG), bulking rate (BR) and density increase rate ($\Delta\rho$) of modified wood are shown in Fig. 1a. The LAR refers to the amount of liquid absorbed by modified wood during the treatment process and is used to evaluate the impregnation effect of wood. The LAR values of all the samples exceeded 200%, indicating that the modified solution of each group fully penetrated the wood. The WPG of the modified wood indicates how much active ingredient remained in the wood after modification [17]. The WPG of the samples treated only by FA was 60.81%, while the WPG of the samples treated by the two-step method was 76.58%, and the improved part was BA/ADP, indicating that the two-step method retained BA/ADP in the wood. The BR refers to the volume increase of wood after modification [18]. The BR value of the BA/ADP-treated sample was 9.15%, indicating that BA and ADP recrystallized in the wood cell walls after drying [13]. The BR values of FA and BA/ADP-FA samples reached 17.31% and 12.81%, respectively, because, during modification, furfuryl alcohol was polymerized and permanently expanded the wood cell walls, thus increasing the volume of the wood [10]. The $\Delta\rho$ indicates changes in wood's density after modification [19]. The $\Delta\rho$ value of the sample treated with BA/ADP-FA reached 56.67%, which was higher than that of the sample treated with BA/ADP (23.89%) because furfuryl alcohol penetrated the cell walls of wood and filled the intercellular spaces after polymerization [20]. This resulted in a greater increase in the density of wood.

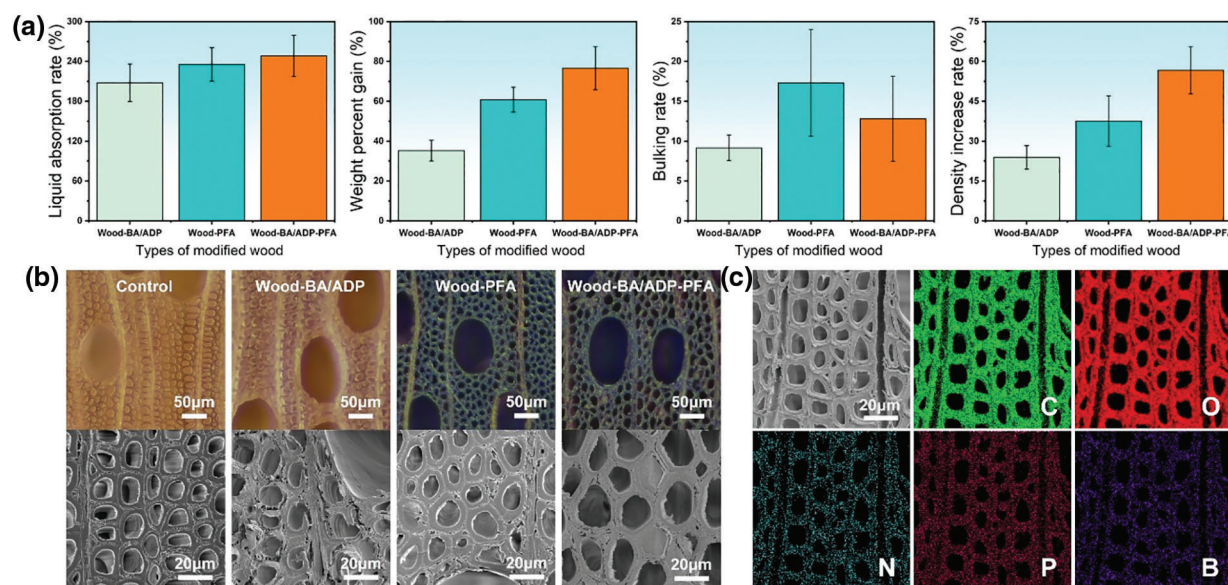


Figure 1: LAR, WPG, BR, and $\Delta\rho$ of the modified wood (a). The micromorphology of the control and modified wood samples (b). EDX element maps showing the elemental distribution of carbon (C), oxygen (O), nitrogen (N), phosphorus (P), and boron (B) of Wood-Ba/ADP-PFA (c)

The morphology and structure of modified wood were characterized by a stereoscopic microscope and SEM (Fig. 1b). The cross-section of the control sample showed irregularly-distributed cell structures, in which large pores were vessels, and small pores were the lumen and were connected to each other and to themselves through the pits [21]. After the first impregnation, white crystals appeared on the inner walls of the lumen of Wood-BA/ADP, and the cell channels were not blocked, which provided favorable

conditions for the impregnation of FA. After the second impregnation, FA was mainly polymerized on the cell walls and the inner walls of the lumen of Wood-BA/ADP-PFA, and only a small number of lumina were blocked, similar to Wood-PFA. This enabled the fabrication of a lightweight modified wood sample and also reduced the consumption of the modification solution and facilitated the passage of water vapor during drying [22]. SEM images showed that the cell walls of the furfurylated wood were significantly thickened, further verifying that large quantities of the FA resin filled the cell walls [23].

To further explore the distribution of BA and ADP in modified wood, EDX analysis was used to detect the elemental composition of Wood-BA/ADP-PFA (Fig. 1c). C and O elements were mainly derived from cellulose, hemicelluloses, and lignin, the main components of wood, and also from the FA resin. P and B elements were derived from ADP and BA. The EDX results showed that the distributions of P and B elements were consistent with the contour of the cell wall, indicating that BA and ADP were fixed in the wood cell walls and the polymerized FA resin [14].

3.2 Physical and Mechanical Properties

Compared with the control sample, the compressive strength of Wood-PFA was 131.61% higher, while that of Wood-BA/ADP-PFA exhibited a greater increase of 166.78% (Fig. 2a). Additionally, the compressive strength of Wood-BA/ADP along the grain showed a modest increase of 107% compared with the control sample. These results underscore the synergistic effect of furfuryl alcohol and BA/ADP on enhancing the compressive strength of modified wood.

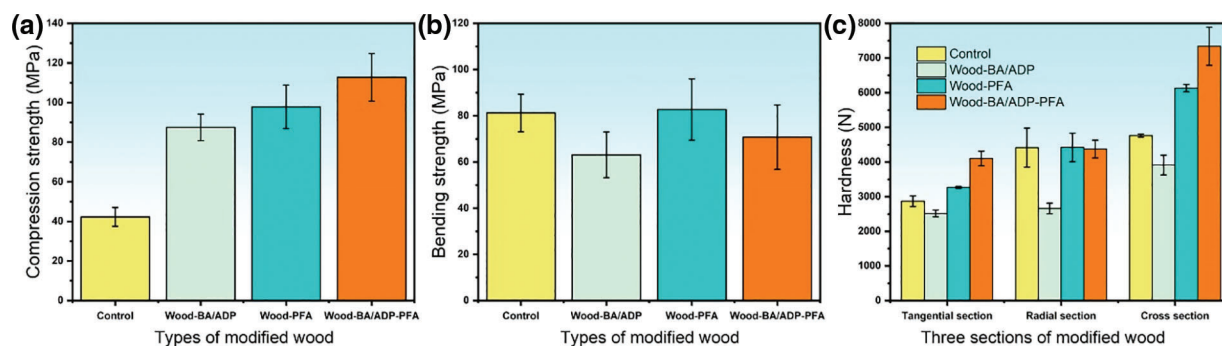


Figure 2: The compressive strength (a), bending strength (b), and hardness of three sections (c) of the control sample and modified wood samples

The bending strength of Wood-PFA exhibited a marginal increase of 1.82% compared with the control sample (Fig. 2b). Conversely, Wood-BA/ADP showed a decrease in its bending strength by 22.33% because the acidity of the BA/ADP modification solution degraded wood during impregnation. Wood-BA/ADP-PFA only displayed a 12.85% decrease in its bending strength compared with Wood-BA/ADP, suggesting that modification with furfuryl alcohol mitigated the decrease in bending strength.

Compared with the control sample, the hardness of Wood-PFA increased by 13.82% and 28.77% in the tangential direction and cross-section, respectively, while showing no significant change in the radial direction (Fig. 2c). This suggests that furfural alcohol modification resulted in an overall enhancement in poplar wood's hardness. Conversely, the hardness of Wood-BA/ADP decreased in all directions, with the most pronounced decrease in the radial direction of 39.76%. This decline in hardness was attributed to the acidic nature of the BA/ADP modification solution, which degraded poplar wood during impregnation. In contrast, the hardness of Wood-BA/ADP-PFA increased by 42.90% and 54.18% in the

tangential direction and cross-section, respectively, compared with the control sample, with no significant change in the radial strength. The trend in hardness change resembled that of Wood-PFA, indicating that the modification's impact on hardness primarily depended on the furfuryl alcohol resin. Additionally, the hardness of Wood-BA/ADP-PFA significantly surpassed that of Wood-PFA due to the mild acidity of BA/ADP, which allowed it to catalyze the modification process. This promoted furfuryl alcohol polymerization and increased the generation and polymerization degree of furfuryl alcohol resin in Wood-BA/ADP-PFA.

3.3 Fixation Properties

The modification process and the interaction between the modifier and the wood were analyzed, resulting in the identification of the possible modifier fixation mechanism (Fig. 3a). Considering the prolonged exposure of modified wood to wet environments, it is imperative to ensure that modifying agents are retained within the wood. Consequently, leachability tests were conducted on modified wood samples, and the results are shown in the Fig. 3b. The leaching rate of Wood-PFA was only 10.94%, which was primarily attributed to the polymerization of furfuryl alcohol into furfuryl alcohol resin within the wood, which formed strong bonds with the wood cell walls. The insolubility of furfuryl alcohol resin rendered it highly resistant to leaching during subsequent water immersion. Conversely, the leaching loss of Wood-BA/ADP was 101.39%, indicating a near-complete loss of the chemical agent. The observed value exceeding 100% suggests that some wood components were also leached alongside the modifier. Notably, the leaching rate of Wood-BA/ADP-PFA was 30.59%, suggesting that furfuryl alcohol modification after BA/ADP modification mitigated the loss of the modifying agent.

To further investigate possible chemical reactions between furfuryl alcohol and wood cell walls, FTIR spectra of the corresponding samples were recorded (Fig. 3c,d). The peak at 3400 cm^{-1} corresponds to the absorption of the -OH stretching vibration of the wood cell walls. The absorption peak at 1599 cm^{-1} was attributed to the vibration of the lignin aromatic skeleton [24]. In furfured wood, this peak became weaker, indicating that furfuryl alcohol reacted with lignin in addition to undergoing *in-situ* polymerization in wood cell walls. It is unclear whether the introduction of BA/ADP affected the polymerization of furfuryl alcohol. The peaks at 1233, 1162, 1059, and 1036 cm^{-1} are the C-H deformation vibration absorption peaks of furan rings. Comparing the spectra of Control and Wood-PFA shows that the Wood-PFA peak was significantly stronger, indicating the successful polymerization of the furfuryl alcohol resin. Comparing the spectra of Wood-BA/ADP-PFA shows that these peaks strength of furan rings was greater than that of Wood-PFA, indicating that furfuryl alcohol had a higher degree of polymerization after the introduction of BA/ADP. This was because both BA and ADP are acidic, and because furfuryl alcohol requires acidic conditions for polymerization, BA/ADP catalyzed its polymerization.

The addition of BA/ADP was confirmed by EDX analysis. To further explore the existence state of the internal components of the modified wood, we analyzed the atomic contents and atomic binding states of the modified wood using XPS. As shown in Fig. 3e, there were many C and O atoms in all samples, and the B and P contents of Wood-BA/ADP and Wood-BA/ADP-PFA were also high, further confirming the addition of BA and ADP. According to the B 1s XPS spectrum (Fig. 3f), the high-intensity peak at 192.4 eV was due to B-O-B bonds, indicating that boric acid was deposited after entering the wood. The O 1s and P 2p spectra show that P atoms mainly existed in O-P-O and O=P bonds, indicating that ammonium dihydrogen phosphate mainly existed as deposits in wood. O=P-O-C bonds were also detected around 135.4 eV, indicating that a minor quantity of ammonium dihydrogen phosphate might have interacted with wood cellulose [25].

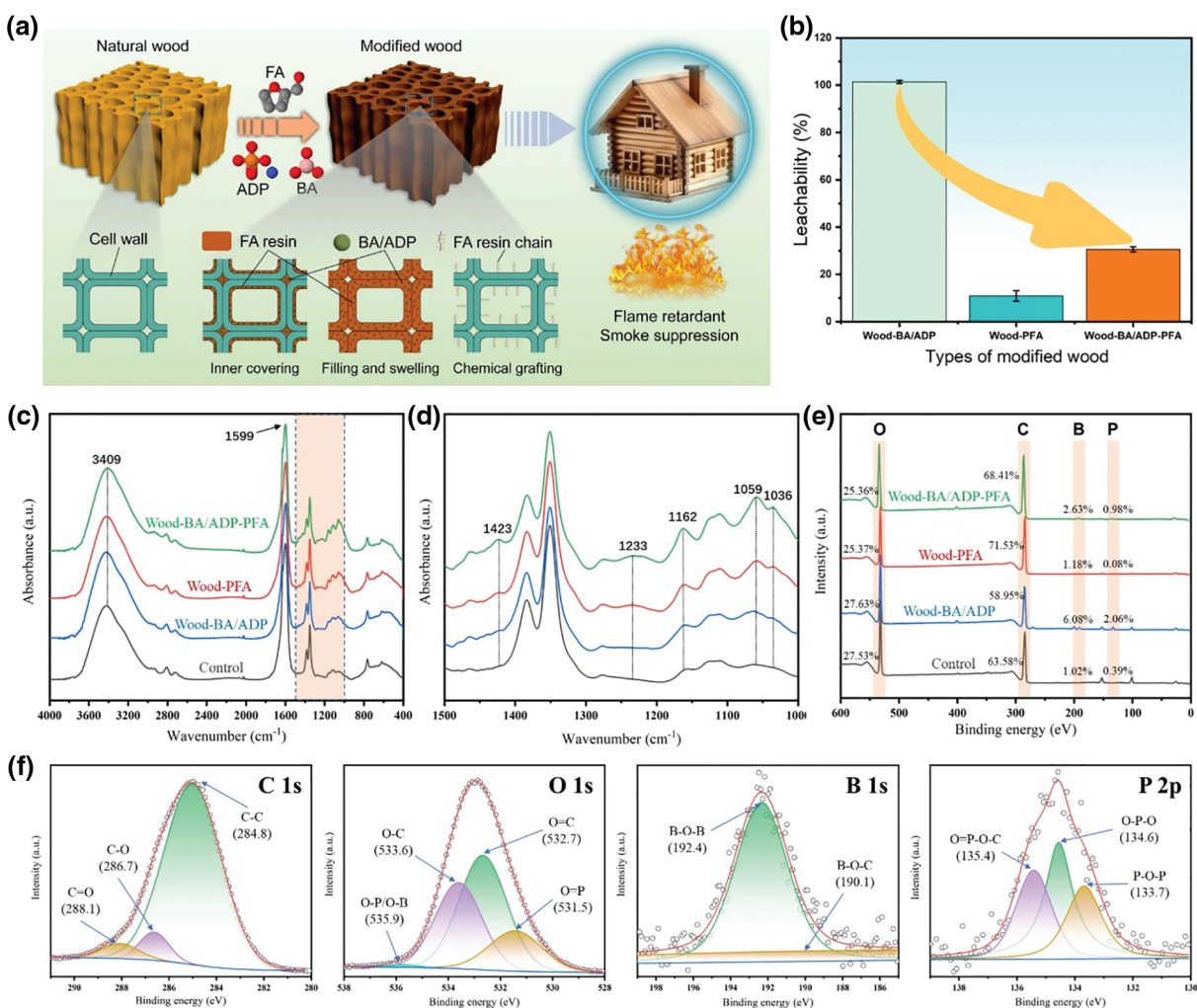


Figure 3: Schematic illustration of the fabrication process and possible fixation mechanism (a) of Wood-BA/ADP-PFA; Leachability (b) of modified wood; FTIR spectra of modified wood at 4000–400 cm⁻¹ (c) and amplified spectra in the region of 1500–400 cm⁻¹ (d); XPS spectra (e) of modified wood; High-resolution C 1s, O 1s, B 1s, and P 2p spectra (f) of Wood-BA/ADP-PFA

3.4 Thermal Stability

Thermogravimetric analysis was employed to assess the thermal stability of the modified wood samples, including TG (Fig. 4a) and DTG (Fig. 4b), with relevant data listed in Table 1. For the unmodified control wood, the loss of absorbed water in the cell walls primarily took place from ambient temperature up to 200°C. As the temperature gradually increased, the wood components began to decompose, leading to a competition between the emission of volatile substances and the development of a stable carbon structure [14]. Among wood components, hemicelluloses have poor thermal stability [15], so they first underwent pyrolysis, and dehydration-carbonization occurred from 200°C to 260°C. Cellulose undergoes pyrolysis at temperatures between 240°C and 370°C. Because cellulose was the most abundant wood component, the primary peak in the DTG curve was ascribed to cellulose pyrolysis [26], and the maximum decomposition rate occurred at 333.35°C. Lignin pyrolysis primarily occurred above 370°C, within the overall temperature range of 280°C–500°C. At 800°C, only 3.33% carbon residue remained in the unmodified control wood sample. The addition of PFA resin delayed wood pyrolysis. Chain cleavage and

decomposition of the PFA resin began at 200°C and involved the cleavage of weaker chemical bonds [27], which slowed the pyrolysis of wood and improved its thermal stability.

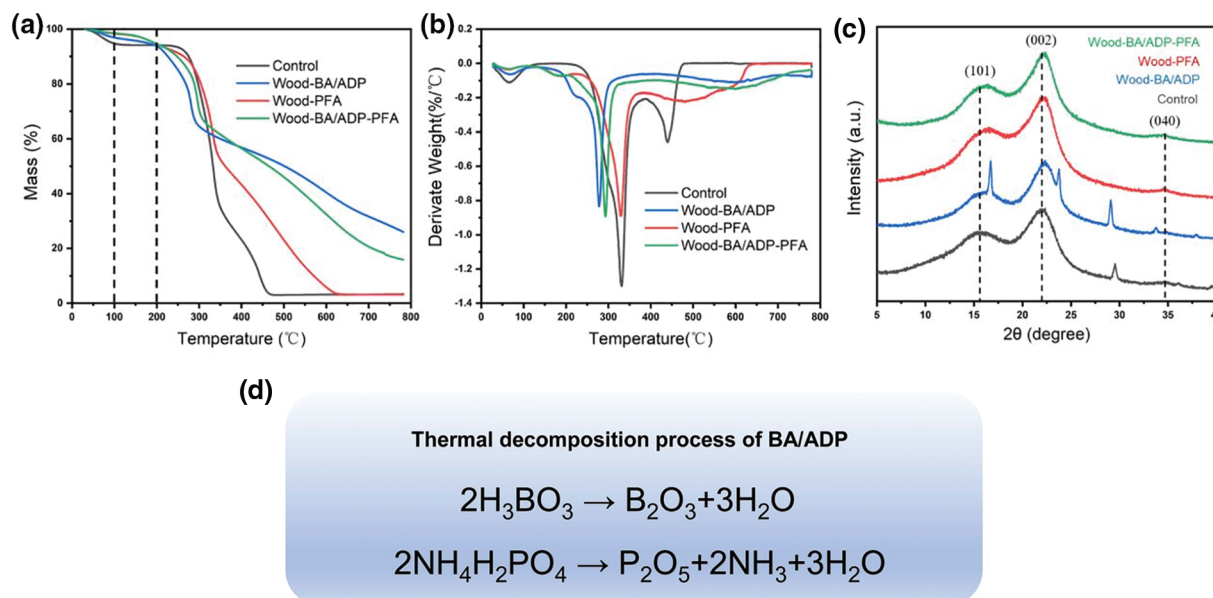


Figure 4: TG (a) and DTG (b) curves of modified wood; XRD pattern (c) of modified wood; Thermal decomposition process of BA and ADP (d)

Table 1: Thermogravimetric analysis data of the control sample and modified wood

Samples	$T_{10\%}^a$ (°C)	T_{\max}^b (°C)	Residue (%)
Control	275.17	333.35	3.33
Wood-BA/ADP	226.13	280.41	26.02
Wood-PFA	263.73	331.44	3.15
Wood-BA/ADP-PFA	247.98	295.16	15.89

The TG and DTG curves of Wood-BA/ADP and Wood-BA/ADP-PFA were highly similar, indicating that BA and ADP were the key factors influencing the pyrolysis process, leading to an increase in wood carbon residues and improving the thermal stability of wood. BA underwent decomposition at approximately 100°C–200°C, forming a protective glass layer (B_2O_3) and releasing water [28]. As the temperature continued to rise, ADP underwent dehydration to produce phosphoric acid ($\text{H}_4\text{P}_2\text{O}_7$), which further condensed into metaphosphoric acid (HPO_3) [29]. At 500°C, metaphosphoric acid formed P_2O_5 and H_2O , resulting in the formation of a glass phase [13]. The possible thermal decomposition processes of BA and ADP are shown in Fig. 4c. The addition of BA and ADP increased the carbon residue amount from 3.15% to 15.89%, effectively enhancing the thermal stability of furfurylated wood.

XRD (Fig. 4d) was conducted to assess the crystallinity of samples before and after modification. All samples exhibited characteristic diffraction peaks at $2\theta = 16^\circ$, 22° , and 34.6° , which corresponded to the (101), (002), and (040) crystal planes of cellulose I. Notably, a broad peak appeared around 18.6° , indicating the amorphous region of cellulose. In comparison to the untreated wood, the peaks corresponding

to the (101) and (002) planes of cellulose I in the pattern of Wood-BA/ADP showed a slight decrease in intensity. This observation was attributed to the acidity of the BA/ADP modification solution, which induced the degradation of celluloses in wood. As shown in Table 2, the relative crystallinity of poplar increased from 49.15% to 56.56% after BA/ADP impregnation. This enhancement was because the BA/ADP solution degraded the amorphous region of cellulose, which increased the overall relative crystallinity. In contrast, the furfuryl alcohol-impregnated samples displayed significantly stronger diffraction peaks corresponding to the (101) and (002) crystal planes. This enhancement suggests an improvement in the crystallinity of cellulose after furfuryl alcohol polymerization. The resulting densification of cellulose's structure may have increased the number of hydrogen bonds formed between neighboring cellulose chains, which restrained thermal expansion and enhanced the thermal stability of samples.

Table 2: Crystallinity characteristics of samples

Samples	I_{002}	I_{amorph}	CrI (%)
Control	4934.9	2509.2	49.15%
Wood-BA/ADP	4661.9	2024.9	56.56%
Wood-PFA	6338.6	3624.4	42.82%
Wood-BA/ADP-PFA	5464.2	2497.5	54.29%

3.5 Flame Retardant Performance

Cone calorimetry tests on both the control and modified wood samples were conducted to simulate combustion during a fire [30]. The main parameters evaluated during the tests included the time to ignition (TTI), heat release rate (HRR), peak heat release rate (PHRR), mean heat release rate (MHRR), total heat release (THR), smoke production rate (SPR), total smoke release (TSR), CO yield (COY), mean CO yield (MCOY), CO₂ yield (CO₂Y), mean CO₂ yield (MCO₂Y), and carbon residue ratio. These values are shown in Fig. 5 and Table 3.

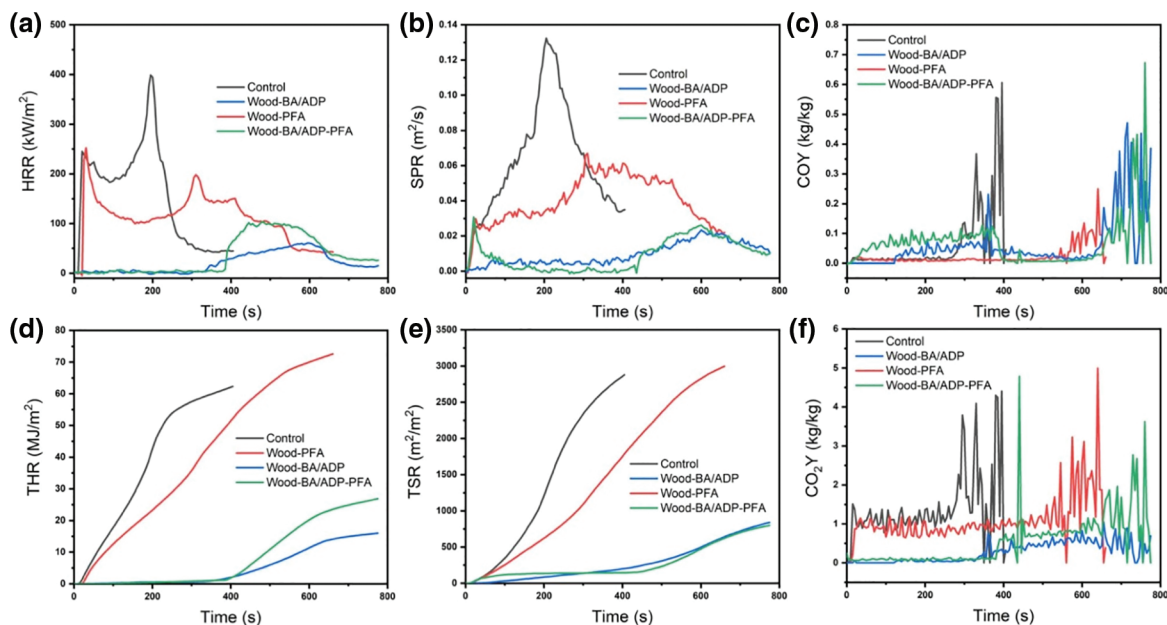


Figure 5: (Continued)



Figure 5: The main combustion parameters (a–f) obtained by cone calorimetry of wood and modified wood, along with a photo (g) showing the residual carbon after combustion

Table 3: Cone calorimetry data of the control and the modified wood samples

Parameter type	Control	Wood-BA/ADP	Wood-PFA	Wood-BA/ADP-PFA
TTI (s)	10	342	18	385
PHRR (kW/m ²)	398.7934	60.8117	252.1795	103.4715
MHRR (kW/m ²)	157.6939	35.2219	113.4161	65.8872
THR (MJ/m ²)	62.2893	15.2072	72.6015	25.6960
TSR (m ² /m ²)	2875.4856	679.2845	2993.2379	652.5562
MCOY (kg/kg)	0.0211	0.0460	0.0130	0.0187
MCO ₂ Y (kg/kg)	1.1425	0.4548	0.9314	0.7686
Residue (%)	16.4700	39.2400	30.1200	42.7800

The samples were heated rapidly during the tests using a conical heater, which initiated the thermal degradation and decomposition reactions that released volatile and combustible species. These species were then ignited by a spark igniter to start the combustion process of the samples [31]. The control wood ignited after 10 s and rapidly hit the initial peak heat release rate (245.19 kW/m²) by emitting a substantial amount of heat. As the combustion progressed, a protective carbon layer developed on the wood surface, resulting in the inhibition of heat release, oxygen penetration, and the discharge of flammable gases, consequently decreasing the heat release rate and leading to the appearance of a trough in the curve (Fig. 5a). HRR reached the second peak (398.79 kW/m²) as the protective carbon layer was broken and a large number of volatile and combustible pyrolysis products were released until the combustible products were exhausted and the control wood was left with crushed ash. The total heat release (THR) of Wood-PFA exceeded that of control wood by 16.56%, suggesting that the incorporation of PFA resulted in greater release of flammable gas and facilitated fire propagation. Towards the conclusion of the test, Wood-PFA yielded more char residue (Fig. 5g).

After adding BA and ADP, Wood-BA/ADP and Wood-BA/ADP-PFA showed difficulty reigniting, and the TTI was greatly delayed to 342 and 385 s, respectively (Table 3). The HRR and THR of both were also significantly reduced (Fig. 5a,d), indicating a significant reduction in the fire growth rate. The glassy protective layer formed through the combustion process involving BA and ADP, as previously discussed, acted as a physical barrier, restricting the transfer of heat and oxygen to the underlying wood. The final

carbon residue rates of Wood-BA/ADP and Wood-BA/ADP-PFA increased to 39.24% and 42.78%, respectively, and the structural integrity, compactness, and strength were higher (Fig. 5g).

In addition to heat release, smoke release is another crucial factor in assessing the combustion performance of materials. The addition of BA and ADP significantly decreased the SPR and TSR of wood (Fig. 5b,e). The TSR of Wood-BA/ADP-PFA was reduced by 77.31% in comparison to the control wood. Compared with the control, the MCOY of Wood-BA/ADP was 118.01% higher due to the formation of a heat-stable carbon layer that protected polysaccharides, inhibited thermal decomposition, and enhanced the production of CO during the smoldering stage. Conversely, the MCOY of Wood-BA/ADP-PFA decreased by 11.37% compared with the control sample, suggesting that further utilization of furfuryl alcohol mitigated the release of CO. The findings demonstrate that the co-modification of BA/ADP and furfuryl alcohol suppressed the formation of flue gas particles and toxic gases by improving the thermal stability of the protective carbon layer.

In other studies, both Kong et al. [14] and Zhang et al. [13] used a one-step method to modify wood with furfuryl alcohol and flame retardants. The peak heat release rate (PHRR) and total heat release (THR) of Wood-BA/ADP-PFA, prepared using the two-step method in this study, were 33.93% and 43.02% lower than those reported in KONG's study, and 33.91% and 53.02% lower than those reported in Zhang's study, respectively. This indicates a significant enhancement in the flame retardant performance of Wood-BA/ADP-PFA prepared in this study compared to the results of similar studies.

4 Conclusions

In this work, BA/ADP flame-retardant furfurylated wood was prepared by a two-step method. According to the results of the weight gain rate and EDX spectrum analysis, BA/ADP was retained in furfurylated wood. The chemical composition analysis showed that BA and ADP mainly existed in their original chemical states, but some ADP may have reacted with furfuryl alcohol. The acidity of BA and ADP promoted furfuryl alcohol polymerization during furfurylation. The increase in the crystallinity of furfuryl alcohol-modified wood indicated that furfuryl alcohol polymerized after entering wood cell walls and expanded cellulose. The addition of BA and ADP increased the thermal stability and carbon residue rate of furfurylated wood. The time to ignition was delayed from 10 to 385 s, and the total heat release and total smoke release decreased by 58.75% and 77.31%, respectively. Furfurylated wood prepared by this two-step method showed excellent fire retardancy and smoke suppression performance, which may help inhibit the spread of fire and reduce damage caused by high-intensity heat and smoke release during actual fires. This material holds promising applications as a construction material in timber buildings. With the increasing demand for fire safety, the research on flame retardancy of indoor materials has great potential.

Acknowledgement: Thanks to the National Joint Engineering Research Center for Green Processing Technology of Agricultural and Forestry Biomass, the Provincial-Ministry Collaborative Innovation Center for Efficient Utilization of Wood and Bamboo Resources, and the Hunan Provincial Key Laboratory of Biomass Materials and Green Conversion Technology for providing scientific research platforms.

Funding Statement: This work was financially supported by the Key Research and Development Program of Hunan Province, China (2023NK2038), National Natural Science Foundation of China (32201485), Natural Science Foundation of Hunan Province, China (2022JJ40863, 2023JJ60161), Scientific Research Project of Hunan Provincial Education Department, China (21B0238, 22A0177) and Hunan Provincial Technical Innovation Platform and Talent Program in Science and Technology, China (2023RC3159).

Author Contributions: Ming Ni: Writing—original draft, Data curation; Lei Li: Data curation; Yiqiang Wu: Methodology; Jianzheng Qiao: Funding acquisition, Project administration; Yan Qing: Investigation; Ping

Li: Funding acquisition, Project administration; Yingfeng Zuo: Writing—review & editing, Methodology, Funding acquisition. All authors reviewed the results and approved the final version of the manuscript.

Availability of Data and Materials: The data from this study can be obtained from the corresponding author (Yingfeng Zuo) upon reasonable request.

Ethics Approval: This study does not include human or animal subjects.

Conflicts of Interest: The authors declare that they have no conflicts of interest to report regarding the present study.

References

1. Gallezot P. Conversion of biomass to selected chemical products. *Chem Soc Rev.* 2012;41(4):1538–58. doi:10.1039/C1CS15147A.
2. Ding Y, Pang Z, Lan K, Yao Y, Panzarasa G, Xu L, et al. Emerging engineered wood for building applications. *Chem Rev.* 2022;123(5):1843–88.
3. Mola-Yudego B, Arevalo J, Diaz-Yanez O, Dimitriou I, Freshwater E, Haapala A, et al. Reviewing wood biomass potentials for energy in Europe: the role of forests and fast growing plantations. *Biofuels.* 2017;8(4):401–10. doi:10.1080/17597269.2016.1271627.
4. Dong Y, Wang K, Li J, Zhang S, Shi SQ. Environmentally benign wood modifications: a review. *ACS Sustain Chem Eng.* 2020;8(9):3532–40. doi:10.1021/acssuschemeng.0c00342.
5. Zheng Y, Zhang R, Zhang L, Gu Q, Qiao Z. A resol-assisted cationic coordinative co-assembly approach to mesoporous ABO₃ perovskite oxides with rich oxygen vacancy for enhanced hydrogenation of furfural to furfuryl alcohol. *Angew Chem Int Edit.* 2021;60(9):4774–81. doi:10.1002/anie.v60.9.
6. An Z, Li J. Recent advances in the catalytic transfer hydrogenation of furfural to furfuryl alcohol over heterogeneous catalysts. *Green Chem.* 2022;24(5):1780–808. doi:10.1039/D1GC04440K.
7. Li X, Jia P, Wang T. Furfural: a promising platform compound for sustainable production of C₄ and C₅ chemicals. *ACS Catal.* 2016;6(11):7621–40. doi:10.1021/acscatal.6b01838.
8. Guigo N, Jerome F, Sousa AF. Biobased furanic derivatives for sustainable development. *Green Chem.* 2021;23(24):9721–2. doi:10.1039/D1GC90124A.
9. Baysal E, Ozaki SK, Yalinkilic MK. Dimensional stabilization of wood treated with furfuryl alcohol catalysed by borates. *Wood Sci Technol.* 2004;38:405–15.
10. Shen X, Yang S, Li G, Liu S, Chu F. The contribution mechanism of furfuryl alcohol treatment on the dimensional stability of plantation wood. *Ind Crop Prod.* 2022;186:115143. doi:10.1016/j.indcrop.2022.115143.
11. Li W, Wang H, Ren D, Yu Y, Yu Y. Wood modification with furfuryl alcohol catalysed by a new composite acidic catalyst. *Wood Sci Technol.* 2015;49(4):845–56. doi:10.1007/s00226-015-0721-0.
12. Martin LS, Jelavic S, Cragg SM, Thygesen LG. Furfurylation protects timber from degradation by marine wood boring crustaceans. *Green Chem.* 2021;23(20):8003–15. doi:10.1039/D1GC01524A.
13. Zhang L, Zhang W, Peng Y, Wang W, Cao J. Thermal behavior and flame retardancy of poplar wood impregnated with furfuryl alcohol catalyzed by boron/phosphorus compound system. *Ind Crop Prod.* 2022;176:114361. doi:10.1016/j.indcrop.2021.114361.
14. Kong L, Guan H, Wang X. *In situ* polymerization of furfuryl alcohol with ammonium dihydrogen phosphate in poplar wood for improved dimensional stability and flame retardancy. *ACS Sustain Chem Eng.* 2018;6(3):3349–57. doi:10.1021/acssuschemeng.7b03518.
15. Zhang L, Xu J, Shen H, Xu J, Cao J. Montmorillonite-catalyzed furfurylated wood for flame retardancy. *Fire Safety J.* 2021;121(13):103297. doi:10.1016/j.firesaf.2021.103297.
16. Lin CF, Karlsson O, Kim I, Myronycheva O, Mensah RA, Försth M, et al. Fire retardancy and leaching resistance of furfurylated pine wood (*Pinus sylvestris* L.) treated with guanyl-urea phosphate. *Polymers.* 2022;14(9):1829. doi:10.3390/polym14091829.

17. Wang J, Yao Y, Huang Y, Ma Y, Xi J, Wang X, et al. Effects of the combination of compression and impregnation with phenolic resin on the dimensional stability in the multiscale wood structure of Chinese fir. *Constr Build Mater.* 2022;327:126960. doi:10.1016/j.conbuildmat.2022.126960.
18. Zhang X, Song S, Li X, Zhu Y, Li X, Xu K, et al. Effect of low molecular weight melamine-urea-formaldehyde resin impregnation on poplar wood pore size distribution and water sorption. *Ind Crop Prod.* 2022;188:115700. doi:10.1016/j.indcrop.2022.115700.
19. Bi X, Zhang Y, Li P, Wu Y, Yuan G, Zuo Y. Building bridging structures and crystallization reinforcement in sodium silicate-modified poplar by dimethylol dihydroxyethylene urea. *Wood Sci Technol.* 2022;56(5):1487–508. doi:10.1007/s00226-022-01414-w.
20. Yang T, Zhang K, Mei C, Ma E, Cao J. Effects of furfurylation on interactions between moisture sorption and humidity conditioning of wood. *Wood Sci Technol.* 2022;56(3):703–20. doi:10.1007/s00226-022-01375-0.
21. Chen C, Kuang Y, Zhu S, Burgert I, Keplinger T, Gong A, et al. Structure-property-function relationships of natural and engineered wood. *Nat Rev Mater.* 2020;5(9):642–66. doi:10.1038/s41578-020-0195-z.
22. Liu MH, Guo F, Wang HK, Ren WT, Cao MD, Yu Y. Highly stable wood material with low resin consumption via vapor phase furfurylation in cell walls. *ACS Sustain Chem Eng.* 2020;8(37):13924–33. doi:10.1021/acssuschemeng.0c03172.
23. Liu MH, Lyu SY, Peng LM, Cai LP, Huang ZH, Lyu JX. Improvement of toughness and mechanical properties of furfurylated wood by biosourced epoxidized soybean oil. *ACS Sustain Chem Eng.* 2021;9(24):8142–55. doi:10.1021/acssuschemeng.1c01358.
24. Xia Q, Chen C, Yao Y, Li J, He S, Zhou Y, et al. A strong, biodegradable and recyclable lignocellulosic bioplastic. *Nat Sustain.* 2021;4(7):627–35. doi:10.1038/s41893-021-00702-w.
25. Deh S, Gähr F, Buchmeiser M. Synergistic effects in the pyrolysis of phosphorus-based flame-retardants: the role of Si- and N-based compounds. *Polym Degrad Stabil.* 2016;130:155–64. doi:10.1016/j.polymdegradstab.2016.06.009.
26. Zhang L, Ran Y, Peng Y, Wang W, Cao J. Combustion behavior of furfurylated wood in the presence of montmorillonite and its char characteristics. *Wood Sci Technol.* 2022;56(2):623–48. doi:10.1007/s00226-022-01369-y.
27. Guigo N, Mija A, Zavaglia R, Vincent L, Sbirrazzuoli N. New insights on the thermal degradation pathways of neat poly(furfuryl alcohol) and poly(furfuryl alcohol)/SiO₂ hybrid materials. *Polym Degrad Stabil.* 2009;94(6):908–13. doi:10.1016/j.polymdegradstab.2009.03.008.
28. Lin CF, Karlsson O, Martinka J, Rantuch P, Garskaite E, Mantanis GI, et al. Approaching highly leaching-resistant fire-retardant wood by *in situ* polymerization with melamine formaldehyde resin. *ACS Omega.* 2021;6(19):12733–45. doi:10.1021/acsomega.1c01044.
29. Liodakis S, Tsapara V, Agiovlasis IP, Vorisis D. Thermal analysis of *Pinus sylvestris* L. wood samples treated with a new gel-mineral mixture of short- and long-term fire retardants. *Thermochim Acta.* 2013;568:156–60. doi:10.1016/j.tca.2013.06.011.
30. Merk V, Chanana M, Gaan S, Burgert I. Mineralization of wood by calcium carbonate insertion for improved flame retardancy. *Holzforschung.* 2016;70(9):867–76. doi:10.1515/hf-2015-0228.
31. Fu Q, Medina L, Li Y, Carosio F, Hajian A, Berglund LA. Nanostructured wood hybrids for fire-retardancy prepared by clay impregnation into the cell wall. *ACS Appl Mater Interfaces.* 2017;9(41):36154–63. doi:10.1021/acsomega.7b10008.